Ca^{2+} Binding to Occluded Sites in the CrATP-ATPase Complex of Sarcoplasmic Reticulum: Evidence for Two Independent High-Affinity Sites†

Carol Coan,* Ji-Ying Ji, and Jose Adalberto Amaral

School of Dentistry, University of the Pacific, 2155 Webster Street, San Francisco, California 94115

Received July 27, 1993; Revised Manuscript Received January 21, 1994®

ABSTRACT: Occluded Ca^{2+} sites in the CrATP-ATPase complex are studied by first forming the complex in the presence of EGTA so that the sites can be occluded while vacant. $^{45}Ca^{2+}$ binding to the occluded sites is then studied under equilibrium conditions. Binding curves are produced for two independent Ca^{2+} sites with $K_d(1) = 0.2$ μM and $K_d(2) = 1.6$ μM. When both sites are saturated, only the Ca^{2+} bound to the lower affinity site can exchange with free Ca^{2+}. On addition of EGTA (15 vs 0.5 mM Ca^{2+}) all bound Ca^{2+} dissociates, the net dissociation rate of one-half of the Ca^{2+} being approximately 10-fold greater than that of the other one-half (at 37 °C). When Ca^{2+} is bound only to the higher affinity site, this Ca^{2+} will exchange slowly if the concentration of free Ca^{2+} is below the saturation level of the lower affinity site. An ionophore dependency of the rates of binding and dissociation indicates that the access to the sites is through the interior of the vesicle. Solubilization in $C_{12}E_9$ releases the Ca^{2+} in the higher affinity site. Our observations are consistent with a model of the ATPase where the lower affinity of two transport sites is associated with the interior position (closest to the lumen) in a transmembrane channel. It is futher evident that when in the occluded state, the higher affinity site is available without Ca^{2+} first being bound to the lower affinity site, eliminating cooperativity from the binding mechanism. In turn, this implies a connection between the integrety of the high-affinity binding site and the linking of sections of the catalytic site by CrATP.

The SR[1] Ca^{2+}-ATPase regulates the Ca^{2+} concentration in the cytoplasm of the muscle cell by actively pumping Ca^{2+} to the interior of the reticulum for storage. The pumping mechanism is triggered when Ca^{2+} binds to two high-affinity sites on the cytoplasmic side of the ATPase, which in turn induces changes in the catalytic site that promote phosphorylation of the enzyme. By this means the cation to be transported initiates the transport process. Following the formation of the phosphoenzyme, the bound Ca^{2+} becomes occluded (Dupont, 1980) and then dissociates to the vesicle lumen in response to a decrease in Ca^{2+} binding affinity [de Meis & Carvalho, 1974; Ikemoto, 1975; Coan et al., 1979; for a review, see Inesi et al. (1992)].

The central role of Ca^{2+} in the activation of the enzyme has made the Ca^{2+} binding sites the subject of considerable study. A structural model, deduced from the primary sequence, hypothesizes the enzyme to consist of a transmembrane channel that is connected to large hydrophilic loops, sections of which comprise the catalytic site (Brandl et al., 1986). Site-specific mutagenesis (Clarke et al., 1989; Vilsen & Andersen, 1992b) and chemical modification (Sumbilla et al., 1991) indicate that at least one of the two Ca^{2+} binding sites may be centrally located within the channel, a minimum of 45 Å from the initial site of ATP binding (Highsmith & Murphy, 1984; Scott, 1985), requiring long-range linkage between the Ca^{2+} sites and the site of catalysis. The Ca^{2+} binding is cooperative (Hill coefficient of 1.8; Inesi et al., 1980), and it is quite well established that the bound Ca^{2+} is exchanged with free Ca^{2+} or dissociated from the high-affinity sites in a sequential order (Ikemoto et al., 1981; Dupont, 1982; Nakamura, 1987; Inesi, 1987; Petithory & Jencks, 1988a,b; Orlowski & Champeil, 1991). There is also evidence that each Ca^{2+} site may have a different role in the mechanism (Fujimori & Jencks, 1992; Champeil, 1993) and that binding to the higher affinity site alone is sufficient to promote phosphorylation (Coan & DiCarlo, 1990). However, the relationship between the two Ca^{2+} sites and their respective roles in controlling the behavior of the catalytic site is not well understood.

A major barrier to obtaining information about the Ca^{2+} sites has been the cooperativity in the binding mechanism, which does not allow the Ca^{2+} to be bound to either site independently of the other. We show here that this problem can be circumvented when CrATP is used in place of MgATP. It has been known for some time that CrATP binds tightly to the ATPase, holding the enzyme in an intermediate step of the transport cycle (Serpersu et al., 1982; Vilsen & Andersen, 1986, 1987, 1992a; Chen et al., 1991). In this state the Ca^{2+} remains bound in an occluded form, which appears to be similar to the Mg·ADP·E-P·Ca_2 species. The stability of the complex comes from the tight binding properties of Cr(III), which bridges segments of the catalytic site and the γ and β phosphates of the bound ATP (Serpersu et al., 1982; Chen et al., 1991). In a preliminary report, we demonstrated that the vacant Ca^{2+} sites can be occluded when the CrATP-ATPase complex is formed in the presence of EGTA and that Ca^{2+} will then bind independently to these sites (Amaral & Coan, 1991). The slow rates of Ca^{2+} binding, dissociation, and exchange allow for a thorough kinetic analysis.

MATERIALS AND METHODS

SR vesicles were prepared from the white skeletal muscle of rabbit hind legs using methods previously described (Eletr & Inesi, 1972). Vesicles were stored in a buffered sucrose

† This work was supported by National Institutes of Health Grant GM38073 and American Heart Association Grant-in-Aid 88007240.

* To whom correspondence should be addressed.

® Abstract published in *Advance ACS Abstracts,* March 1, 1994.

[1] Abbreviations: SR, sarcoplasmic reticulum; ISL, *N*-(1-oxy-2,2,6,6-tetramethyl-4-piperidinyl)iodoacetamide; MOPS, 3-(*N*-morpholino)-propanesulfonic acid; $C_{12}E_9$, poly(oxyethylene) 9-lauryl ether.

0006-2960/94/0433-3722$04.50/0

medium (30% sucrose and 10 mM MOPS, pH 6.8) at 4 °C and were used within 4–5 days of preparation. ATP, phosphoenolpyruvate, lactic dehydrogenase, pyruvate kinase, bovine serum albumin, and ionophore A23187 were purchased from Sigma. ISL [*N*-1-oxy-2,2,6,6,-tetramethyl-4-piperidinyl)iodoacetamide] was purchased from Molecular Probes, and $^{45}Ca^{2+}$ was purchased from ICN.

Protein concentrations were measured using folin reagent according to the techniques of Lowry et al. (1951) using bovine serum albumin as a standard. In certain cases protein concentrations were also determined from the absorbance at 280 nm using an OD of 1.05 cm^{-1} for 1 mg of SR protein in 1 mL of 1% sodium dodecyl sulfate (Thorley-Lawson & Green, 1973). These procedures generally agreed to within 10%. ATPase activity was monitored using a coupled assay system with pyruvate kinase (8 μg/mL), phosphoenolpyruvate (1 mM), lactate dehydrogenase (220 μg/mL), and NADH (100 μg/mL) (Anderson & Murphy, 1983). The assay medium contained 10 mM $MgCl_2$, 2 mM EGTA, 2 mM $CaCl_2$, 100 mM MOPS, pH 6.8, 80 mM KCl, 1 μg/mL ionophore A23187, 5 mM ATP, and approximately 10 μg/mL SR. Activities of our SR preparations are typically 4–4.5 μmol min^{-1} mg^{-1} at 25 °C.

Preparation of CrATP. The heating method of preparation of bidentate CrATP, followed by purification with Dowex 50-H^+ at 4 °C, was used precisely as described by Cleland (1982). $HClO_4$, 0.5 M, was used to elute the bidentate CrATP. Following elution, the solution was adjusted to pH 3.8 with saturated $KHCO_3$. HPLC techniques were used to check the purity of the preparation, and we typically found 90–95% of the nucleotide to be γ, β-CrATP. The remaining nucleotide was divided between ATP, ADP, AMP, and tridentate CrATP.

Formation of CrATP–ATPase. SR, 1–2 mg/mL, was incubated with given concentrations of bidentate CrATP at 37 °C for 90 min or the time specified in a given experiment (100 mM MOPS, pH 6.8, 80 mM KCl, 5 μg ionophore A23187 per milligram of protein, $CaCl_2$, and EGTA as specified). To follow the formation of the CrATP–ATPase complex, 5 μL of the incubation mixture was added to 1 mL of activity assay at given times, and the hydrolysis of ATP was measured. The Cr–enzyme bond is irreversible in the time of an activity measurement, and it was assumed that the 5 mM ATP in the activity assay quenched the CrATP interaction. Measurements were taken at 25 °C.

To measure occluded Ca^{2+}, an aliquot of a given CrATP–SR incubation (usually 100 μL; conditions of individual experiments are given in the figure captions) was diluted into 1 mL of cold buffer (10 mM $MgCl_2$, 10 mM MOPS, and 8 mM KCl, pH 6.8) and SR was collected by vacuum filtration through a Millipore filter (type HAWP, prewashed with 5 mL of cold buffer). The SR on the filter was then washed with 25 mL of the cold buffer, and the filter was submerged in 5 mL of Opti-Fluor (Packard) and allowed to sit for 12 h (overnight) before radiocounting. As a control, the volume of the wash was varied; by 15 mL the Ca^{2+} that remained with the SR had leveled to approximately 8 nmol/mg of SR protein, and this level remained constant to 60 mL, at which point the experiment was terminated. Twenty-five milliters was chosen as a median value. As an additional control, 1 mM $CaCl_2$ was added to the 1 mL of dilution medium, and as long as the medium remained cold (4 °C) and the sample did not sit longer than 1–2 min, there was no apparent loss of bound Ca^{2+}. In all experiments, background measurements were obtained from aliquots taken 5–10 s after the addition of CrATP. Background counts per minute were less than 10% of those of a typical sample.

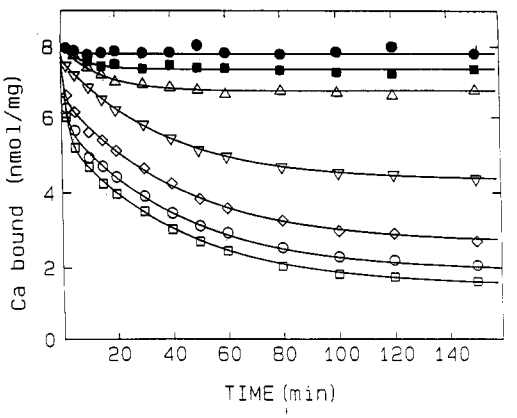

FIGURE 1: Dissociation of Ca^{2+} from the CrATP–ATPase complex. EGTA was added to solutions of SR vesicles that had been incubated with 480 μM CrATP, 500 μM EGTA, and 500 μM $^{45}CaCl_2$ (16 μM free $^{45}Ca^{2+}$) for 90 min at 37 °C. Incubation medium contained 1 mg/mL SR, Mops buffer (100 mM Mops and 80 mM KCl, pH 6.8), and 0.5 μg of ionophore A23187/mL. The EGTA concentrations were chosen so that the final free $^{45}Ca^{2+}$ concentrations were 0.017 (□), 0.026 (○), 0.053 (◇), 0.26 (▽), 2.6 (△), 5.7 (■) and 16 μM (●). At the specified times aliquots were diluted into cold Mops buffer containing 10 mM $MgCl_2$ for filtration and washing as described in Materials and Methods. The best fit (solid lines) to a two-site model (eq 1) gave $K_{d(fast)} = 0.031 \pm 0.001$ μM, $k_{off(fast)} = 0.39 \pm 0.02$ min^{-1}, $K_{d(slow)} = 1.23 \pm 0.04$ μM, and $k_{off(slow)} = 0.022 \pm 0.001$ min^{-1}, where the two sites are defined by their relative rates of dissociation. The data sets given here were obtained on two preparations of SR with the same preparation of CrATP. The amount of bound calcium at $t = 0$ varied between 7.8 and 8.1 nmol per milligram of SR protein. Data points were omitted to prevent clutter. The standard error in reproducing a given data point fell between 0.3 and 0.5 nmol/mg.

Alternatively, samples were placed on the top of 1-cc syringes with small cotton plugs containing G-50 Sephadex gel (Penefsky, 1977). The samples were collected by a 30-s centrifugation in a bench-top low-speed centrifuge, and radiocounts were determined. Before the samples were added, the columns were centrifuged for 1 min to remove all excess buffer.

EPR Spectroscopy. A Bruker ER-200D EPR spectrometer (X-band) interfaced to an IBM S-9001 computer was used with IBM EPR application software for all experimental measurements and data analysis. To measure the ISL–ATPase spectrum, a 40 mg/mL SR sample was used, with a modulation amplitude of 2 G, 19 mW of power, an 80-ms time constant, and a 200-s sweep of 100 G.

Fitting Procedures. Kinetic and equilibrium parameters were obtained by fitting the following equations with BASIC computer programs that employ nonlinear regression algorithms (Bevington, 1969). These programs were provided by Dr. Alexander Murphy. To describe the dissociation of Ca^{2+} from two independent sites at various free Ca^{2+} concentrations (Figure 1), the equation

$$\frac{[Ca]_{bound}}{P} = \frac{[E]_{total}}{P}\sum_{i=1}^{i=2}\left(\frac{[Ca^{2+}]/K_{d(i)} + \exp[-([Ca^{2+}]K_{d(i)} + 1)k_{off(i)}t]}{[Ca^{2+}](K_{d(i)} + 1)}\right) \quad (1)$$

where $[Ca]_{bound}/P$ is the concentration of bound calcium (nmol) per milligram of total protein and $[E]_{total}$ is the total

concentration of CaATPase, was solved for values of $k_{off(i)}$ and $K_{d(i)}$ (the dissociation rate constants and equilibrium constants, respectively). To describe Ca^{2+} dissociation from a single site at a given free Ca^{2+} concentration, the equation

$$\frac{[Ca]_{bound}}{P} = \frac{[Ca]^{f}_{bound}}{P} + \left(\frac{[Ca]^{0}_{bound} - [Ca]^{f}_{bound}}{P}\right) \exp(-k_{off}t) \quad (2)$$

was solved for k_{off}, $[Ca]^{f}_{bound}/P$, and $[Ca]^{0}_{bound}/P$ (nmol of initial and final bound calcium, respectively, per milligram of protein). Best-fit values of k_{off} and $[Ca]^{f}_{bound}/P$ are given in the figure captions and in the text where appropriate. In all cases best-fit values of $[Ca]^{0}_{bound}/P$ were very close to experimental values (as is evident by the y-axis intercepts of the fitted curves) and were not listed separately. To describe equilibrium binding, the equation

$$\frac{[Ca]_{bound}}{P} = \sum_{i=1}^{i=2} \left(\frac{[Ca^{2+}][Ca]^{f}_{bound(i)}}{P(K_{d(i)} + [Ca^{2+}])}\right) \quad (3)$$

was solved for values of $K_{d(i)}$ and $[Ca]^{f}_{bound(i)}$ (the dissociation constant and the amount of calcium bound to each site at saturation).

RESULTS

Dissociation of Ca^{2+} from the CrATP–ATPase·Ca_2 Complex. Following incubation of the SR Ca-ATPase with CrATP (a 90-min incubation at 37 °C with 16 μM free $^{45}Ca^{2+}$ and 5 μg of ionophore A23187 per milliter), we find that 7.9 ± 0.2 nmol of $^{45}Ca^{2+}$ per milligram of SR, or 2 Ca^{2+} per ATPase, is not removed by extensive washing with cold buffer.[2] The addition of 10 mM Mg^{2+} to the wash buffer, which helps remove loosely bound calcium (Inesi et al., 1980), does not decrease the measured amount of trapped $^{45}Ca^{2+}$, nor does the addition of 1–2 mM $^{40}Ca^{2+}$ as long as the buffer is cold and the exposure time is short (see Materials and Methods). Since ionophore A23187 allows for the rapid equilibration of calcium across the membrane, we conclude that the trapped $^{45}Ca^{2+}$ is truly occluded and, from the stoichiometry, that both of the high-affinity sites on the ATPase are saturated. However, when EGTA is added to the 37 °C incubation medium, a slow dissociation of the occluded $^{45}Ca^{2+}$ can be observed. In the experiments shown in Figure 1, varying amounts of EGTA were added to reduce the $^{45}Ca^{2+}$ concentration to levels that should partially saturate the high-affinity sites. The dissociation is biphasic, and the faster of the two phases appears to be eliminated at higher $^{45}Ca^{2+}$ concentrations. When the $^{45}Ca^{2+}$ concentration is very low, each phase releases about half of the occluded $^{45}Ca^{2+}$. The data in Figure 1 are very similar to those presented by us in a preliminary report (Amaral & Coan, 1991) and to those presented by Vilsen and Andersen (1992a), except that in the latter case the SR was diluted into varying concentrations of $^{40}Ca^{2+}$. In Figure 1, as well as in the preliminary report, we fit the data with a function describing two sites with differing dissociation constants and rates of dissociation, as follows (where site 1 = fast and site 2 = slow):

$$\begin{array}{l} \text{CrATP–E}\begin{matrix}\text{Ca} \\ \text{Ca}\end{matrix} \xrightarrow[k_{off(fast)}]{} \text{CrATP–E}\begin{matrix}\text{Ca} \\ \end{matrix} + Ca^{2+}\text{ ("off" fast site)} \\ \text{CrATP–E}\begin{matrix}\text{Ca} \\ \text{Ca}\end{matrix} \xrightarrow[k_{off(slow)}]{} \text{CrATP–E}\begin{matrix} \\ \text{Ca}\end{matrix} + Ca^{2+}\text{ ("off" slow site)} \end{array} \quad (4)$$

This treatment assumes that the release from each site is independent of the degree of saturation of the other site and that an equilibrium is reached where the amount of Ca^{2+} remaining on each site is determined by the respective K_d. The best fit was obtained with $K_{d(fast)} = 0.031$ μM, $k_{off(fast)} = 0.39$ min^{-1}, $K_{d(slow)} = 1.23$ μM, and $k_{off(slow)} = 0.022$ min^{-1}, where k_{off} is the net dissociation constant. This is the simplest treatment that takes into consideration a difference in binding site affinity, and it is evident from the fit to the data that this treatment can account for the variation in the slopes and the end points of the time courses.

On the other hand, Ca^{2+} dissociation from the native enzyme is thought to be sequentially ordered, and it is likely that both Ca^{2+} sites are aligned in a channel (Inesi, 1987; Petithory & Jencks, 1988a; Orlowski & Champeil, 1991). A sequentially ordered dissociation would trap a fraction of the Ca^{2+} at the more occluded site when the less occluded site was partially saturated, and this too could lead to variations in observed dissociation rates and to a higher apparent binding affinity for the more occluded site (Petithory & Jencks, 1988a). In Figure 1 the dissociation of the first Ca^{2+} is too fast to determine whether the second Ca^{2+} dissociates concomitantly, but the best-fit values for the K_d's are lower than those of the native enzyme (Inesi et al., 1980). Vilsen and Andersen (1992a) found that they could fit their data, which was obtained at a lower temperature, with a sequential model as well as with an independent-site model, but they did not take into consideration the difference in site affinity. We show below (Figures 2–7) that two different dissociation constants need to be taken into account. Also, we cannot eliminate a more complex mechanism where the rate constant and the K_d of an individual site change with the degree of saturation of the other site (a true cooperative mechanism). In order to fit the data with more than one release rate for a given site and to take into consideration the difference in affinity, a minimum of six parameters is required, which is not appropriate for the number of independent variables in these experiments.

It can be concluded from the data in Figure 1, as well as from the data of Vilsen and Andersen (1992a), that Ca^{2+} remains tightly bound to the enzyme when trapped in the occluded state and that one of the two binding sites is more occluded than the other, but given a difference in site affinity, it is difficult to distinguish sequential dissociation, or to determine the relative positions or properties of the two sites. To do this, we need a means of observing the behavior of each site individually.

Ca^{2+} Binding to the CrATP–ATPase Complex. We have shown previously that the formation of the of CrATP–ATPase does not require Ca^{2+} to be bound to the enzyme (Chen et al., 1991). In Figure 2we demonstrate that when $^{45}Ca^{2+}$ is added to CrATP–ATPase that was initially formed without Ca^{2+} in the medium, the rate of binding of the added $^{45}Ca^{2+}$ is very slow. We interpret this to mean that the vacant Ca^{2+} sites were occluded when the CrATP–ATPase complex was formed. Time courses are given in Figure 2 at two free $^{45}Ca^{2+}$ concentrations, one that should saturate both sites (16 μM) and one that should direct Ca^{2+} primarily to the higher affinity site (0.18 μM). In contrast to the dissociation (Figure 1), both time courses were monophasic and could be described by a single-exponential function, with a given net rate of

[2] The average of 24 measurements, obtained from the data sets presented in the figures. The stoichiometry of the ATPase is taken as 4–4.5 nmol per milligram of protein, based on the maximal level of phosphoenzyme we obtain in our preparations.

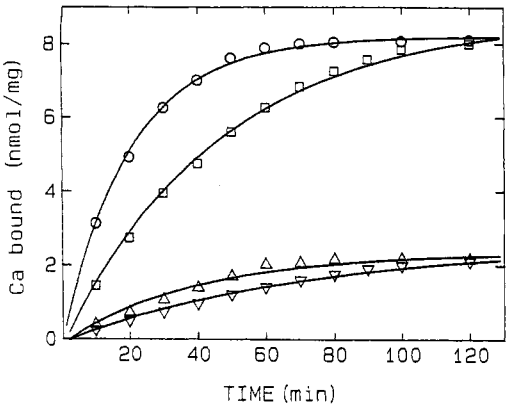

FIGURE 2: Rate of Ca^{2+} binding to the CrATP–ATPase complex. $^{45}CaCl_2$, 500 (○, □) or 125 μM (△, ▽) was added to a 1 mg/mL SR solution which had first been incubated with 480 μM CrATP and 500 μM EGTA for 90 min at 37 °C (free $^{45}Ca^{2+}$ concentrations were 16 and 0.18 μM, respectively). The incubation medium also contained Mops buffer (100 mM Mops, pH 6.8, and 80 mM KCl) and 0.5 μg of ionophore A23187/mL (○, △) or no ionophore (□, ▽). At the specified times aliquots were diluted into cold Mops buffer containing 10 mM $MgCl_2$ for filtration and washing. In some experiments (□, ▽) ionophore was added to the dilution media immediately after the SR to release free Ca^{2+} that was trapped inside the vesicles. Solid lines give the fits to the data with an exponential function describing binding to one or more sites at the same rate (an algebraic arrangement of eq 2 to account for an increasing slope). The rate constants for the data sets were k_{on}(○) = 0.048 ± 0.001 min^{-1}, k_{on}(□) = 0.021 ± 0.001 min^{-1}, k_{on}(△) = 0.025 ± 0.004 min^{-1}, and k_{on}(▽) = 0.014 ± 0.002 min^{-1}. Values of $[Ca]^f_{bound}/P$ were (○) 8.2 ± 0.1, (□) 8.7 ± 0.2, (△) 2.4 ± 0.1, (▽) 2.6 ± 0.2 nmol/mg. The data sets in the figure were obtained from the same preparation of CrATP–ATPase. For comparative purposes, separate sets were obtained on another SR preparation. Parameters agreed within experimental error.

binding. This rate was higher at the higher Ca^{2+} concentration [k_{on}(16 μM) = 0.048 min^{-1} vs k_{on}(0.18 μM) = 0.025 min^{-1}], but the difference in rate was less than the difference in concentration. For comparative purposes, a time course was obtained with 1 mM $^{45}Ca^{2+}$, and this curve was also monophasic with an increase in rate that was smaller than the increase in concentration [k_{on}(1 mM) = 0.071 min^{-1}; data not shown]. For a simple second-order reaction the difference in rate should be directly proportional to the difference in concentration, demonstrating here that an unobstructed collision between the free $^{45}Ca^{2+}$ and the binding site is not the rate-limiting factor.

When ionophore was eliminated from the medium, the rate of binding decreased by a factor of 2 with both 0.18 and 16 μM $^{45}Ca^{2+}$ present (Figure 2). This difference in rate is consistent with the time of passive influx through the bilayer of the SR vesicle and indicates that Ca^{2+} binding occurs from the luminal side of the membrane.

When the maximum level of occluded calcium was determined over a wide range of free $^{45}Ca^{2+}$ concentrations, the binding curve shown in Figure 3 was produced. The best fit was obtained with the sum of two hyperbolic functions (eq 3), representing two independent binding sites with a $K_d(1)$ of 0.14 μM and a $K_d(2)$ of 1.65 μM, respectively. For comparative purposes a fit is also given for a single hyperbolic function (dashed line in Figure 3a). This fit would correspond to two sites with identical dissociation constants (K_d = 0.7 μM), and while there is not a large difference in the two fits, the curve generated by the single hyperbolic function fits through few of the experimental points (the experimental error in measuring a given data point is approximately 5%). However, the difference in binding affinities is much more apparent when exchange properties are measured.

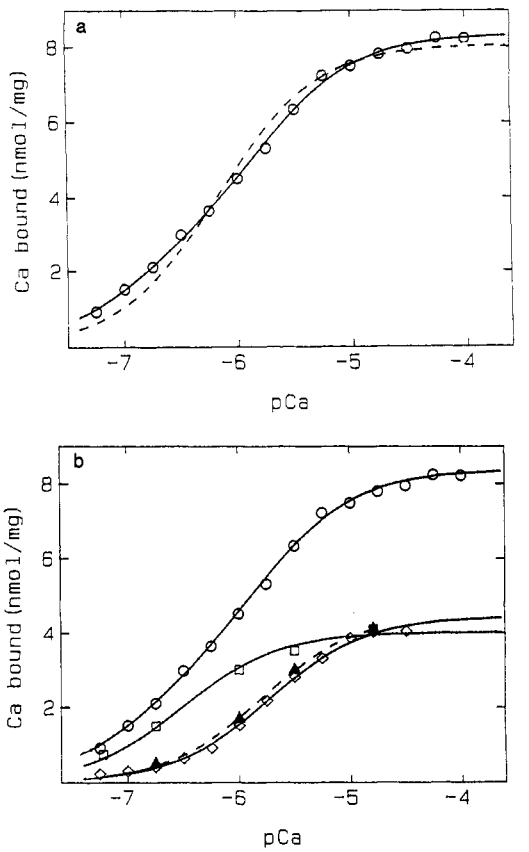

FIGURE 3: Ca^{2+} binding to the CrATP–ATPase complex as a function of free Ca^{2+} concentration. Varying amounts of $^{45}CaCl_2$ (to give the indicated free $^{45}Ca^{2+}$) were added to aliquots from an SR solution that had first been incubated with 480 μM CrATP and 500 μM EGTA for 90 min at 37 °C. The incubation medium contained 1 mg/mL SR, Mops buffer (100 mM Mops, pH 6.8, and 80 mM KCl), and 0.5 μg of ionophore A23187/mL. After a second 90-min incubation with the $^{45}Ca^{2+}$ present, the aliquots were diluted into cold Mops buffer containing 10 mM $MgCl_2$ for filtration and washing. In the ○ data set (panels a and b) there were no further additions. The solid line through this set gives the best fit to the sum of two hyperbolic functions (eq 3), which define a binding site where $K_d(1)$ = 0.14 ± 0.05 μM and $[Ca]^f_{bound}$ $(1)/P$ = 3.3 ± 0.7 nmol/mg and a binding site where $K_d(2)$ = 1.6 ± 0.3 μM and $[Ca]^f_{bound}(2)/P$ = 5.0 ± 0.4 nmol/mg. In panel a, the dashed line gives the best fit to the single-site form of eq 3 where K_d = 0.71 ± 0.07 μM and $[Ca]^f_{bound}/P$ = 8.1 ± 0.1 nmol/mg. In panel b, in the experiments designated by □, 10 mM $^{40}CaCl_2$ was added after the 90-min incubation with varying amounts of $^{45}CaCl_2$, and the solution was incubated for an additional 60 min before dilution and washing. The solid line through this data set gives the best fit to the single-site form of eq 3 where K_d = 0.25 ± 0.02 μM and $[Ca]^f_{bound}/P$ = 4.5 ± 0.2 nmol/mg. The ▲ data set gives the difference between data set □ and data set ○; the dashed line gives the best fit where K_d = 1.58 ± 0.04 μM and $[Ca]^f_{bound}/P$ = 4.5 ± 0.5 μM. In the data described by ◇ experimental conditions were exactly as described for the set given by ○ except that the ATPase had been solubilized in $C_{12}E_9$ before the initial incubation with CrATP. The solid line through this set gives the best fit with the single-site form of eq 3 where K_d = 1.9 ± 0.1 μM and $[Ca]^f_{bound}/P$ = 4.3 ± 0.1 μM. The standard error in reproducing a point at a given concentration was approximately 0.5 nmol/mg.

Exchange of Occluded $^{45}Ca^{2+}$ with Excess $^{40}Ca^{2+}$. The proposed sequential dissociation mechanism for the native enzyme is based in part on the observation that one-half of the bound Ca^{2+} will exchange with Ca^{2+} in the extravesicular medium more rapidly the other half (Dupont, 1982; Nakamura, 1987; Inesi, 1987; Petithory & Jencks, 1988a; Orlowski & Champeil, 1991). By forming CrATP–ATPase·$^{45}Ca_2$ complexes in the manner described in Figure 3, we can observe exchange at varying degrees of saturation of the two binding sites. In the experiments shown in Figure 4, 0.18, 1.0, 3.2,

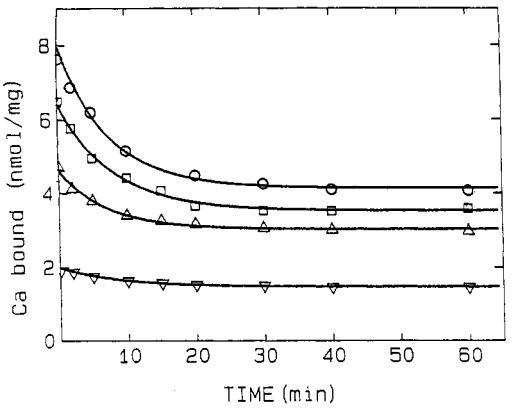

FIGURE 4: Exchange of occluded $^{45}Ca^{2+}$ in partially saturated CrATP–ATPase with excess $^{40}Ca^{2+}$. An SR solution was first incubated with 480 μM CrATP and 500 μM EGTA for 90 min and then divided into separate solutions, which were incubated for 80 min with $^{45}CaCl_2$ to give free $^{45}Ca^{2+}$ of 0.18 (▽), 1.0 (△), 3.2 (□), 16 μM (○). At t = 0, 10 mM $^{40}CaCl_2$ was added to each solution. At the specified times aliquots were diluted into cold Mops buffer containing 10 mM $MgCl_2$ for filtration and washing. The incubation medium (37 °C) contained 1 mg/mL SR, Mops buffer (100 mM Mops, pH 6.8, and 80 mM KCl), and 0.5 μg of ionophore A23187/mL. Solid lines give the best fits to the data with eq 2. Best fit rate constants for the dissociation of the $^{45}Ca^{2+}$ were k_{off}(0.18 μM) = 0.12 ± 0.01 min^{-1}, k_{off}(1 μM) = 0.14 ± 0.01 min^{-1}, k_{off}(3.2 μM) = 0.13 ± 0.01 min^{-1}, and k_{off}(16 μM) = 0.14 ± 0.01 min^{-1}. The data given here was one of two sets. Reproducibility was within experimental error.

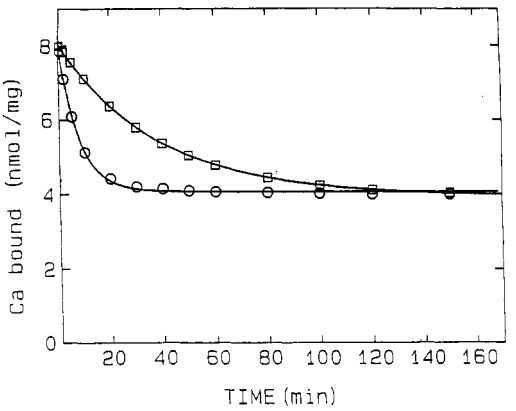

FIGURE 5: Ionophore dependency of Ca^{2+} exchange. Ten millimolar $^{40}CaCl_2$ was added to SR solutions that had been incubated for 60 min with 480 mM CrATP, 500 μM $^{45}CaCl_2$, and 500 μM EGTA (16 μM free $^{45}Ca^{2+}$). Incubation medium contained 1 mg/mL SR, 100 mM Mops, pH 6.8, and 80 mM KCl, at 37 °C. At the specified times aliquots were diluted into cold Mops buffer containing 10 mM $MgCl_2$ for filtration and washing. In the time course described by ○, 0.5 μg of ionophore A23187/mL was in the incubation medium; in □ the ionophore was omitted from the incubation medium (both incubations) but was added to the dilution medium immediately before filtration. Solid lines give the best fit to the data with eq 2 where k_{off} = 0.13 ± 0.02 min^{-1} with ionophore and k_{off} = 0.025 ± 0.003 min^{-1} without ionophore in the incubation. The data given in the figure is one of three sets.

or 16 μM $^{45}Ca^{2+}$ was first incubated with CrATP–ATPase and then 10 mM $^{40}Ca^{2+}$ was added for a second incubation. The loss of the bound $^{45}Ca^{2+}$ was followed as this calcium exchanged[3] with the added $^{40}Ca^{2+}$:

$$\text{CrATP–E}\cdot{}^{45}\text{Ca}_2 \xrightleftharpoons{k_{off}} \text{CrATP–E}\cdot{}^{45}\text{Ca} + {}^{45}\text{Ca}^{2+} + \text{excess}\,{}^{40}\text{Ca}^{2+} \xrightleftharpoons{k_{on}} \text{CrATP–E}\cdot{}^{45}\text{Ca}\cdot{}^{40}\text{Ca} \quad (5)$$

In eq 5 exchange at only one site is considered. This assumption is justified by the data in Figure 4: when 0.18 μM $^{45}Ca^{2+}$ was initially bound, very little exchange occurred, even after extensive incubation; as the degree of saturation increased, a larger fraction of the $^{45}Ca^{2+}$ exchanged; and when both sites were saturated, exactly one-half of the bound $^{45}Ca^{2+}$ exchanged. A good fit was obtained with a single-exponential function at all concentrations (eq 2), and values of k_{off} were similar (best-fit parameters are given in the caption to Figure 4).

When the amount of remaining occluded $^{45}Ca^{2+}$ was plotted as a function of the $^{45}Ca^{2+}$ concentration in the initial incubation (the initial degree of binding site saturation), a single-site binding curve resulted. This curve was well fit with a single hyperbolic function with a K_d of 0.25 μM (□ in Figure 3b), which is similar to the K_d predicted for the higher affinity site in the two-site fit (Figure 3a). In turn, the amount of $^{45}Ca^{2+}$ that was able to exchange, determined by the difference between the remaining bound $^{45}Ca^{2+}$ and the initial bound $^{45}Ca^{2+}$, produced a binding curve with a K_d of 1.58 μM (▲, broken line in Figure 3b).

When exchange experiments of the type shown in Figure 4 were repeated without ionophore in the membrane, a slower rate of dissociation of the bound $^{45}Ca^{2+}$ was observed. If both sites were saturated, it made no difference if the Ca^{2+} was added before or after the CrATP–ATPase was formed. For comparative purposes the CrATP–ATPase·Ca_2 complex in Figure 5 was prepared with Ca^{2+} initially bound to the enzyme (the ○ data set can be compared to the ○ data set in Figure 4). Exchange was also followed after the addition of 1 mM $^{40}Ca^{2+}$, with and without ionophore, and the rates of dissociation were similar (0.10 and 0.022 min^{-1}, respectively; data not shown).

Several observations can be made from the data presented in this section. First, when high extravesicular Ca^{2+} is added, bound Ca^{2+} will dissociate and be replaced by the extravesicular Ca^{2+} at only one site, the lower affinity site. Ionophore dependency indicates that dissociation occurs through the luminal side, as did binding (Figure 2). Second, the ability to distinguish between the sites by their exchange properties provides strong evidence of two distinct occluded sites on the CrATP–ATPase complex with different affinities for Ca^{2+}. Third, it is evident that the formation of the CrATP–ATPase complex made the higher affinity site available without the need to first bind Ca^{2+} to the lower affinity site, and thus the cooperativity in the binding mechanism has been eliminated.

It should also be noted that the K_d predicted for the higher affinity site in Figure 3a is considerably lower than that predicted in Figure 1, but it is very similar to that of the native enzyme (Inesi et al., 1980). In Figure 3 the dissociation constants were obtained from equilibrium binding measurements and should be reasonably accurate for this occluded state. The pattern of limited dissociation with high external Ca^{2+} is typical of a sequential mechanism, and as discussed in the previous section, the treatment of the data in Figure 1 might be expected to yield an artificially low K_d for the more occluded site, which would be the higher affinity site in these experiments. The K_d for the lower affinity site, $K_d(2)$, is similar in both treatments.

Exchange of Occluded $^{45}Ca^{2+}$ with Equimolar $^{40}Ca^{2+}$. In the dissociation experiments described above 10 mM $CaCl_2$ was added, a concentration that would readily saturate all

[3] It is assumed that the bound $^{45}Ca^{2+}$ slowly dissociates and binds in a state of equilibrium. It is then assumed that the added 10 mM $^{40}Ca^{2+}$ will bind preferentially, separating the equilibrium into two experimentally distinguishable steps.

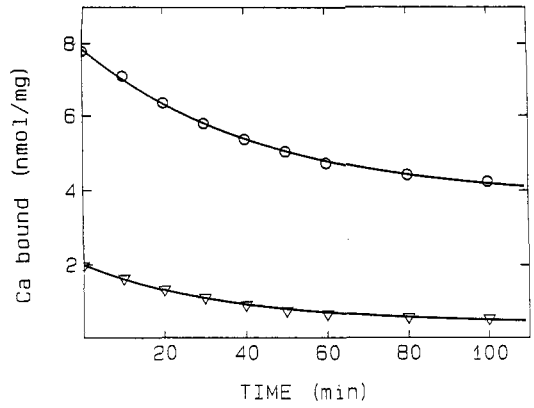

FIGURE 6: Exchange of occluded $^{45}Ca^{2+}$ in partially saturated CrATP–ATPase with equimolar $^{40}Ca^{2+}$. An SR solution, which had first been incubated with 480 μM CrATP and 500 μM EGTA for 90 min, was divided into separate solutions, which were then incubated for 80 min with $^{45}CaCl_2$ to give either 0.18 (○) or 16 μM (▽) free $^{45}Ca^{2+}$. At $t = 0$, the solutions were diluted 5-fold into $^{40}CaCl_2$ so that the final concentration of $^{40}Ca^{2+}$ was the same as the initial concentration of $^{45}Ca^{2+}$. At the specified times aliquots were diluted into cold Mops buffer containing 10 mM $MgCl_2$ for filtration and washing. The incubation medium (37 °C) contained 1 mg/mL SR, Mops buffer (100 mM Mops, pH 6.8, and 80 mM KCl), 0.5 μg of ionophore A23187/mL. Solid lines give the best fit to eq 2 where k_{off}(0.18 μM) = 0.029 ● 0.002 min^{-1} and k_{off}(16 μM) = 0.023 ± 0.001 min^{-1}.

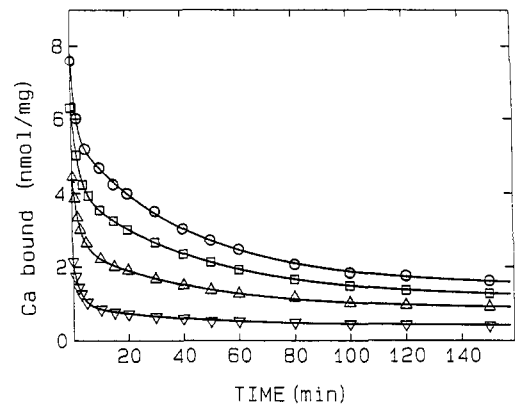

FIGURE 7: Dissociation of occluded Ca^{2+} from the partially saturated CrATP–ATPase complex. An SR solution was first incubated with 480 μM CrATP and 500 μM EGTA for 80 min and then divided into separate solutions to which $^{45}CaCl_2$ was added to give either 0.1 (▽), 1 (△), 3.2 (□), or 16 μM (○) free $^{45}Ca^{2+}$, and the solutions were incubated for an additional 90 min. The incubation media (37 °C) contained 1 mg/mL SR, Mops buffer (100 mM Mops and 80 mM KCl, pH 6.8), and 0.5 μg of ionophore A23187/mL. At $t = 0$, 15 mM EGTA was added, and at the specified times aliquots were diluted into cold Mops buffer containing 10 mM $MgCl_2$ for filtration and washing. Solid lines give the fits to a two-site model with $k_{off(fast)}$ = 0.39 ± 0.04 min^{-1} and $k_{off(slow)}$ = 0.022 ± 0.02 min^{-1} and with the fraction of Ca^{2+} on each site estimated from the data in Figure 5.

available sites. In Figure 6 we show that when $^{45}Ca^{2+}$ is bound primarily to the higher affinity site (0.18 μM $^{45}Ca^{2+}$ was initially added to the CrATP–ATPase) and the SR is then diluted 5-fold into a similar concentration of $^{40}CaCl_2$, the $^{45}Ca^{2+}$ slowly exchanges with the non-radiolabeled Ca^{2+}. This demonstrates that when the lower affinity site is vacant, the higher affinity site can exchange with Ca^{2+} in the extravesicular medium, as long as this Ca^{2+} concentration is also too low to saturate the lower affinity site. A similar exchange was then performed with 16 μM Ca^{2+}, and as is shown in Figure 6, only half of the bound $^{45}Ca^{2+}$ could be exchanged, as with millimolar external Ca^{2+}. However, the dissociation rate was much slower than with millimolar Ca^{2+}.

Dissociation of Ca^{2+} from the Partially Saturated CrATP–ATPase·Ca_2 Complex. When an excess of EGTA is added to SR containing CrATP–ATPase that is partially saturated with $^{45}Ca^{2+}$, we can distinguish between the rates of dissociation of the different sites without complications from the binding of extravesicular Ca^{2+}. As is shown in Figure 7, when the saturation level is low, 80% of the occluded Ca^{2+} dissociates at a rate close to that predicted for the fast population in Figure 1. At full saturation a biphasic dissociation is observed that is identical to that shown in the bottom curve in Figure 1. To fit data at intermediate levels of saturation, estimations of the percentage of Ca^{2+} on the higher and lower affinity sites had to be made. When the data from Figure 3 was used to obtain these estimates, the time courses could be fit very well with the two rates of dissociation obtained in Figure 1 assuming that the high-affinity site is the fast-dissociating site. The ability to fit the data in this manner provides several important controls. First, it demonstrates that the same occluded state is obtained when the Ca^{2+} is bound to the CrATP–ATPase as when it is bound before the complex is formed. Second, we can observe dissociation from the highest affinity site directly, and we find this dissociation rate to be close to that predicted by the fit to the full set of data in Figure 1. Third, it should be noted that the fit to the data is quite sensitive to the assumed fraction of Ca^{2+} released at each rate, and an adequate fit could not be obtained if these fractions differed significantly from those obtained in Figure 3. Finally, it should be noted that our observations are not consistent with cooperative release of the Ca^{2+}, in that when the degree of saturation of the two sites varied, there was no evidence of change in the dissociation rates of the individual sites.

Occlusion of Ca^{2+} in Solubilized CrATP–ATPase. It has been reported that the bound Ca^{2+} remains occluded within the CrATP–ATPase when the complex is solubilized in detergent (Vilsen & Andersen, 1986, 1987). However, we found that only 4 nmol/mg remained occluded when our preparations were solubilized in $C_{12}E_9$. Excess reagents were separated from the solubilized CrATP–ATPase by centrifugation through a G-50 Sephadex column (see Materials and Methods). The time on the column was short (30 s to 1 min), and there was no observed dependency on the time in the detergent, either before or after centrifugation. Isolation of SR vesicles containing CrATP–ATPase by these techniques consistently produced 7.5–8.0 nmol of occluded Ca^{2+} per milligram of protein. The 4 nmol/mg stoichiometry of the solubilized complex was independent of the method of formation, in that we could start with intact vesicles containing 8 nmol/mg occluded Ca^{2+} and then solubilize in detergent or we could form the CrATP–ATPase·Ca^{2+} with the solubilized ATPase. We also repeated these experiments under conditions similar to those of Vilsen and Andersen (1992a; incubation for up to 12 h in 50 mM Tes/Tris, pH 7.0, at 20 °C before dilution into detergent) and obtained the 4 nmol/mg stoichiometry. The difference, then, may well be in the method of separation. Vilsen and Andersen used HPLC to separate the CrATP–ATPase complex from excess reagents, and the higher pressure may have helped to stabilize the occluded Ca^{2+}.

In order to characterize the occluded Ca^{2+} in our preparations, the dissociation rate of $^{45}Ca^{2+}$ was measured following the addition of 10 mM $^{40}Ca^{2+}$ and in the presence of varying concentrations of EGTA. All of the occluded $^{45}Ca^{2+}$ could be replaced by the $^{40}Ca^{2+}$ (●, Figure 8) with $k_{off} = 0.14\ min^{-1}$, which is close to the rate observed with intact vesicles (Figure 4). With EGTA, dissociation was observed when free Ca^{2+}

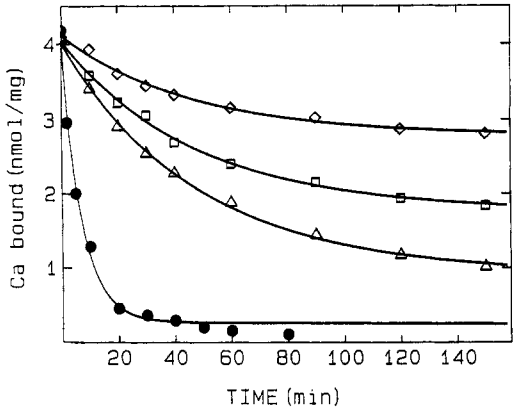

FIGURE 8: Exchange and dissociation of occluded Ca^{2+} in the solubilized CrATP–ATPase complex. Either 10 mM $^{40}CaCl_2$ (●) or varying amounts of EGTA were added to a solution of solubilized ATPase which had been incubated with 480 μM CrATP and 500 μM ^{45}Ca-EGTA (16 μM free $^{45}Ca^{2+}$) for 60 min at 37 °C. At the specified times aliquots were centrifuged on G-50 Sephadex columns as described in Materials and Methods. Following the addition of EGTA, free $^{45}Ca^{2+}$ concentrations were 0.56 (△), 1.33 (□), and 3.16 μM (◇). Solid lines give the best fit to eq 2, where for the addition of 10 mM $^{40}CaCl_2$, k_{off} = 0.14 ● 0.01 min^{-1}, and for the addition of EGTA, k_{off}(0.56 μM) = 0.021 ± 0.01 min^{-1}, k_{off}(1.33 μM) = 0.021 ± 0.01 min^{-1}, and k_{off}(3.6 μM) = 0.022 ± 0.01 min^{-1}.

concentrations were reduced to the range of the lower affinity site (0.52, 1.33, and 3.16 μM in Figure 8). As opposed to that for the dissociation from the intact vesicles, the time courses were monophasic and could be well described by a single-exponential function (eq 2) with the same dissociation rate constant at all concentrations (k_{off} = 0.21 min^{-1}).

In an alternate approach, the experiments of the type described in Figure 3 were repeated with solubilized CrATP–ATPase. The binding curve that was produced is given in Figure 3b, and it is very similar to the curve estimated for the low-affinity site in vesicular SR (◇ vs ▲ in Figure 3). The rate of binding of Ca^{2+} to the solubilized CrATP–ATPase was 0.045 min^{-1}, which is close to that observed with the SR.

Heat Stability of the CrATP–ATPase·Ca_2 Complex. The data described in the previous section suggests that there is a difference in the stability of the two Ca^{2+} bound to the occluded sites. Figure 9a demonstrates the effect of incubations (80 min) at increasing temperatures on the ability of the complex to retain the occluded Ca^{2+}. As is shown in Figure 9, 4 nmol of Ca^{2+} per milligram of protein was lost from vesicular SR as the incubation temperature increased from 40 to 49 °C. Above 49 °C all Ca^{2+} was rapidly lost and the SR became turbid, indicating precipitation of the SR proteins. The enzyme activity was lost between 40 and 49 °C, concomitant with the loss of the first half of the Ca^{2+}. To investigate the effect of temperature on the conformation of the enzyme, shape changes in the EPR spectrum of iodoacetamide-spin-labeled ATPase were followed over the same temperature range (Figure 9b). The shape changes observed in the spectrum were consistent with peptide unfolding (Inesi & Landgraf, 1970). The iodoacetamide spin label (ISL) is known to be sensitive to the conformation of the catalytic site, showing a constriction in the motion of the label when substrate is bound to the enzyme and further constriction when Ca^{2+} binds to the high-affinity sites (Coan & Inesi, 1977; Coan et al., 1979; Inesi, 1980; Lewis & Thomas, 1992). The latter change is thought to correspond to the Ca^{2+}-induced conformational changes that lead to phosphorylation. However, ISL is located on Cys 674 (Wawrzynow et al., 1993), at some distance from the ATP binding site (approximately 60 Å;

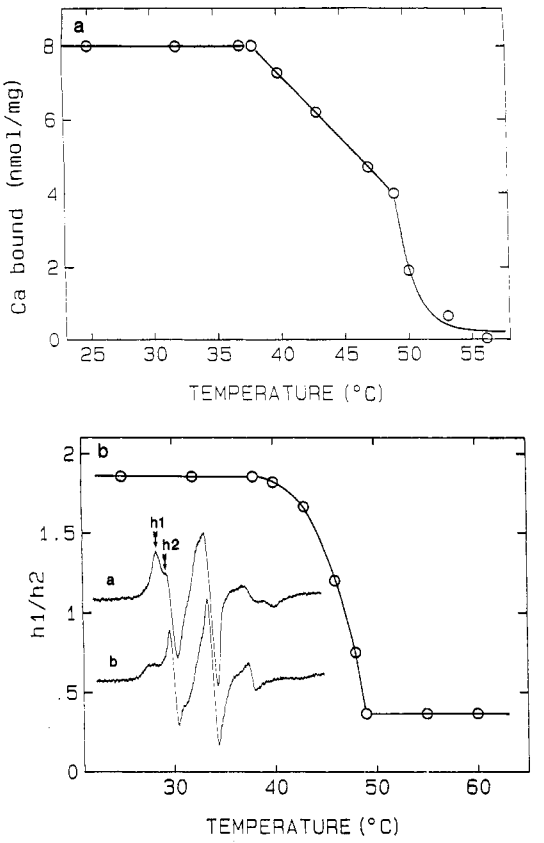

FIGURE 9: Stability of occluded Ca^{2+} and changes in the EPR spectrum of ISL–ATPase as a function of temperature. In panel a, solutions of SR, which had first been incubated with 480 μM CrATP, 500 μM EGTA, and 500 μM $^{45}CaCl_2$ for 90 min at 37 °C, were incubated for 80 min at the indicated temperatures before dilution into cold Mops buffer containing 10 mM $MgCl_2$ for filtration and washing. The radiocounts of the remaining $^{45}Ca^{2+}$ were measured. In panel b, SR with ISL bound to Cys 674 was incubated for 90 min at the indicated temperatures, and then the ratio of two lines in the EPR spectrum, h_1/h_2, was measured. (Panel b, inset) The SR was incubated at 37 °C in spectrum a and at 48 °C in spectrum b. The two lines (h_1 and h_2) are indicated in the spectra. Spectra were measured at room temperature.

Squire et al., 1987), and it is quite possible that the spin label senses the folding of the large hydrophilic loops into an active conformation. The loss of structure around this label concomitant with the loss of one-half of the Ca^{2+} may indicate an interdependency between one of the Ca^{2+} sites and the proper folding.

DISCUSSION

Our ability to form a CrATP–ATPase complex with Ca^{2+}-depleted enzyme has allowed the vacant Ca^{2+} transport sites to be trapped in an occluded state while retaining their high binding affinity. A unique feature of this complex is the ability of Ca^{2+} to bind to the one site of the two with the higher affinity while the site with the lower affinity[4] remains vacant. In all other conditions where the transport sites have been studied in the high-affinity form, Ca^{2+} must first bind to the one with the lower affinity, introducing cooperativity into the mechanism. This has prevented either site from being studied individually. From the data presented here a fairly clear picture of the two occluded sites emerges (K_d(1) = 0.14–0.25

[4] The lower affinity site refers to the K_d = 1.65 vs 0.2 μM site. This should not be confused with the low Ca^{2+} affinity form of the enzyme, which precedes Ca^{2+} release, where the K_d for both sites is in the millimolar range.

μM and $K_d(2)$ = 1.65 μM, respectively, from panels a and b of Figure 3). The K_d of the lower affinity site is an order of magnitude lower than that estimated by fits to the cooperative binding curve (approximately 14 μM; Inesi et al., 1980; Coan & DiCarlo, 1990), while the K_d of the higher affinity site is approximately the same. With the CrATP tightly bound to the enzyme, the access to the sites appears to be from the luminal side of the membrane, and when the lower affinity site is saturated, access to the higher affinity site is blocked, indicating that the lower affinity site is closer to the luminal face. Information provided by this data on the structure and the mechanism of Ca^{2+} binding can be summarized as follows.

Location and Accessibility of the High-Affinity Ca^{2+} Binding Sites. The data presented here is very consistent with the lower affinity Ca^{2+} site being located in the more interior position in a transmembranous channel. Initially, the development of rapid mixing and rapid filtration techniques led to observations at low temperatures of biphasic dissociation of bound Ca^{2+} (Ikemoto et al., 1981) and differences in rates of exchange with free Ca^{2+} (Dupont, 1982). Inesi (1987) was then able to demonstrate at ambient temperature that the more rapidly exchanging Ca^{2+} is the first to be released to the external medium when the enzyme cycle is reversed by the addition of ADP, and that the slower exchanging Ca^{2+} is the first to be transported to the interior of the vesicle in the normal pumping mechanism. Nakamura (1987) was able to demonstrate that ATP binding increases the degree of protection of the slower exchanging site, as does the degree of saturation of the more rapidly exchanging site. Following these studies, Petithory and Jencks (1988a,b) and Orlowski and Champeil (1991) presented quite conclusive evidence that this behavior is due to ordered, sequential binding and release from two sites that differ in their access to the extravesicular media. In all cases, it was noted that the observed behavior would be typical of two single-file sites in a narrow pore or channel, as suggested by positioning the sites in the putative channel in the model of Maclennan and co-workers (Clarke et al., 1889; Vilsen & Andersen, 1992b). However, in the previous studies the observed exchange properties could not be identified with a specific Ca^{2+} site. In our experiments it is very clear that the Ca^{2+} on the higher affinity site is trapped by the Ca^{2+} on the lower affinity site. The assignment of the lower affinity site to the lower (luminal side) position follows from the ionophore dependency of the rates of binding to the occluded sites (Figure 2) and of rates of dissociation in the exchange experiments (Figure 5). A similar ionophore dependency for La^{2+} exchange has recently been reported (Cantilina et al., 1993).

Another observation that is unique to CrATP–ATPase is the degree of protection of the higher affinity Ca^{2+}. In the studies cited above both bound Ca^{2+} ions were able to exchange, the difference being in the rates of exchange, which were much faster than the rates observed here (i.e., 60 and 0.6 s^{-1}, 25 °C; Petithory & Jencks, 1988a), and that the ions were exchanged to the cytoplasmic side of the membrane (Orlowski & Champeil, 1991). Evidently, the tight binding of CrATP to segments of the catalytic site has essentially eliminated access through the hydrophilic portion of the enzyme, allowing only for very slow release through the luminal side, perhaps better described as a slippage through a closed exit. Moreover, we see that Ca^{2+} is able to migrate through the channel from the higher affinity site when the lower affinity site is vacant (Figure 6). Assuming that both are sequentially ordered in a channel, the inability of this Ca^{2+} to exchange with lower affinity Ca^{2+}, even after extensive incubation (Figure 4), must mean that the channel is too narrow to allow the two ions to exchange positions. Accordingly, the exchange to the cytoplasmic side, which was favored under most conditions used by previous investigators, must be with the higher affinity Ca^{2+}, and the Ca^{2+} released to the lumen following phosphorylation (Inesi, 1987) must be from the lower affinity site. As similar half-site behavior is observed in all cases, it appears that the channel characteristics are very similar when the channel is approached from either side.

The positioning of the lower affinity site in the lower position is also consistent with an increase in affinity (i.e., the K_d being decreased from 14 to 1.6 μM) when the channel is tightly closed and with the retention of this site when the ATPase is solubilized in detergent (Figure 9), since this site would be in a structurally rigid and protected region. Squire et al. (1990) have suggested that one of the Ca^{2+} sites may be located close to the top of the channel or in the "stalk" of helices that protrudes above the membrane. Our observations indicate that this would be the higher affinity site, and the location of this site in a region that may be more flexible than the center of the helical cluster is again consistent with this site being less stable in the solubilized enzyme.

Rates of Binding and Dissociation. Two types of kinetic measurements were made here: rates of binding to the occluded sites and rates of dissociation when an excess of either EGTA or $^{40}Ca^{2+}$ was added. Interesting differences were found in the concentration dependencies and monophasic vs biphasic behavior of these rates.

The rate of Ca^{2+} binding was monophasic over a wide range of Ca^{2+} concentrations (18 μM to 1 mM), irrespective of the final degree of saturation of the two sites (Figure 2), and the increase in rate was not proportional to the increase in concentration. This is quite different from the biphasic pattern of dissociation we observed, but it is consistent with two sites that are aligned single file in a channel if the higher affinity site is higher in the channel, as blocking by the lower affinity site would not be expected at concentrations that would permit binding to the higher affinity site. Then taking into consideration that binding is likely to be a two-step process, access of Ca^{2+} to a channel opening (a second-order collision) followed by migration to a given binding site, the relatively small increase in the binding rate observed in Figure 2 (a 2-fold increase in rate vs a 100-fold increase in concentration) might be expected if the second step were rate limiting. Again, to minimize a second-order concentration dependency a channel would have to be sufficiently narrow to limit the increase in internal Ca^{2+} concentration as the external concentration increased, or there would need to be some type of gating mechanism that we have yet to understand.

On the other hand, we saw evidence of a high Ca^{2+} concentration effect on the dissociation rate of the lower affinity site. Dissociation from a given site should be first order, but when millimolar Ca^{2+} was added, the dissociation rate was an order of magnitude higher than when the SR was diluted into 16 μM free Ca^{2+} (Figure 6), although in both cases the dissociation was from the lower affinity site. We have no experimental data that can explain why this happens, but one explanation might be the presence of millimolar binding sites close to the opening of the channel (Jencks, 1992; Jencks et al., 1993; Meszaros & Bak, 1993) that might increase the access to the bound Ca^{2+}. With the possible exception of these high-Ca^{2+} effects, there is no need to invoke any form of cooperativity, other than that implied by the physical requirement that only one Ca^{2+} be able to move through the channel at a time, to explain the data in our experiments.

Cooperativity in the Ca^{2+} Binding Mechanism and Enzyme Activation. Clearly there must be a difference in the Ca^{2+} binding mechanism with CrATP to account for the loss in cooperativity. With the native enzyme, cooperativity follows not just from a sequential binding order but from Ca^{2+} first binding to the lower affinity site, a change in conformation then making the higher affinity site available (Inesi et al., 1980; Fernandez-Belda et al., 1984):

$$E + Ca^{2+} \longrightarrow E{\cdot}Ca_{low} \longrightarrow E'{\cdot}Ca_{low} + Ca^{2+} \longrightarrow E'{\cdot}Ca_{low}{\cdot}Ca_{high} \quad (6)$$

A second conformational change follows substrate binding, providing final control over the transfer of the ATP γ phosphate (Coan & Inesi, 1977; Pickart & Jencks, 1982; Petithory & Jencks, 1988b). The Ca^{2+} sites are not occluded before the $_aE$ conformation is established:

$$E'{\cdot}Ca_2 + MgATP \rightarrow MgATP{\cdot}E'{\cdot}Ca_2 \rightarrow MgATP{\cdot}{}_aE{\cdot}Ca_2 \quad (7a)$$

$$MgATP{\cdot}{}_aE{\cdot}Ca_2 \rightarrow MgADP{\cdot}{}_aE{-}PCa_{2(occluded)} \quad (7b)$$

In the protocol used here the $_aE$ conformation appears to follow Cr(III) chelation, whether or not Ca^{2+} is bound to the enzyme, the further binding of Ca^{2+} being passive and following the order of the binding affinity:

$$E + CrATP \longrightarrow CrATP{\cdot}E \longrightarrow ADP{\cdot}{}_a\overset{Cr}{E{-}P} \quad \text{(occluded vacant sites)} \quad (8a)$$

$$ADP{\cdot}{}_a\overset{Cr}{E{-}P} + Ca^{2+} \longrightarrow ADP{\cdot}{}_a\overset{Cr}{E{-}P}{\cdot}Ca_{high} + Ca^{2+} \longrightarrow$$

$$ADP{\cdot}{}_a\overset{Cr}{E{-}P}{\cdot}Ca_{high}Ca_{low} \quad (8b)$$

This follows not only from the fact that the sites become occluded with the CrATP interaction, but from previous work with the iodoacetamide spin label. The same initial spectral change is observed with CrATP as with MgATP binding, but as the tight Cr(III) bonds form with the enzyme, the conformational change that normally requires Ca^{2+} becomes apparent in the spectrum (Chen et al., 1991). It should also be noted that the dissociation and exchange properties, as well as the binding affinities in the occluded complex, are similar whether Ca^{2+} is bound to the enzyme before or after the CrATP interaction.

With MgATP as the substrate, the $_aE$ conformation is thought to align the ATP binding site and the phosphorylation site. Interactions with the Mg^{2+} and the ribose hydroxyl groups may stabilize this conformation (Coan et al., 1993). In addition, Mg^{2+} is a cofactor in the phosphorylation reaction, and when Ca^{2+} binds to the high-affinity sites, the affinity for Mg^{2+} in the catalytic site increases by about an order of magnitude, with (Reinstein & Jencks, 1993) or without ATP (Coan et al., 1993). It would seem, therefore, that the tight bonds formed between chromium and the enzyme may be able to stabilize the complex under the lower affinity conditions, shifting the enzyme into an "$_aE$ type" conformation. It is difficult to determine whether the enzyme is actually phosphorylated because of the strength of the chromium bonds. However, McIntosh and co-workers (McIntosh et al., 1991; McIntosh, 1992; Ross et al., 1991) have been able to demonstrate that simply linking the phosphorylation domain to the ATP binding domain with a glutaraldehyde cross-bridge will partially occlude the Ca^{2+} sites and hold the enzyme in an ADP-sensitive conformation.

Once the correct conformation has been established, phosphorylation by MgATP is rapid (1000 s^{-1}; Stahl & Jencks, 1987) and a ternary complex with the metal bridging both phosphates and the enzyme would be very short lived. Thus, the CrATP–ATPase complex, with both sides of the channel tightly closed, may be more representative of a transition state than of one of the steady-state intermediates in the cycle, and this may be the major reason that dissociation occurs more rapidly and to the cytoplasmic side from the MgADP·E–P·Ca_2 complex. Nonetheless, the binding affinity measurements, the positioning, and the relative degree of occlusion (i.e., the ability of a given site to exchange from one side of the membrane or to dissociate more rapidly) should be applicable to the occluded forms of both the CrATP and MgATP complexes.

Simply placing the lower affinity Ca^{2+} site in the lower position in a restricted channel implies not only that the higher affinity Ca^{2+} site is not fully intact above the this site in the native enzyme but that the bridge formed between CrATP and the enzyme that closes the channel must provide an alternate means of forming the higher affinity site. Two observations then follow: a direct link appears to exist between the higher affinity binding site and the structural integrity of the catalytic site, and the sequence of events employed with CrATP may be the reverse of the normal order, where the binding of the second Ca^{2+} would control the catalytic site conformation. Tanford et al. (1987) have stressed the advantage of a step by step procession, where one binding event triggers the next, giving precise control over phosphorylation and tightly coupled transport stoichiometry, although their mechanism did not require cooperative binding. The data presented here gives strong support to a mechanism where Ca^{2+} binding to the lower affinity site causes alignment of the channel helices to form the higher affinity site, Ca^{2+} binding to which triggers the conformational change that aligns substrate moieties with reactive groups within the catalytic site.

REFERENCES

Amaral, J., & Coan, C. (1991) *Biophys. J. 59*, 44a.

Anderson, K. W., & Murphy, A. J. (1983) *J. Biol. Chem. 258*, 14276–14278.

Bevington, P. R. (1969) *Data Reduction and Error Analysis for the Physical Sciences*, McGraw-Hill, New York.

Brandl, C. J., Green, N. M., Korczak, B., & MacLennan, D. H. (1986) *Cell 44*, 597–607.

Cantilina, T., Sagara, Y., Inesi, G., & Jones, L. (1993) *J. Biol. Chem. 268*, 17018–17025.

Champeil, P. (1993) *Biophys. J. 64*, A353.

Chen, Z., Coan, C. R., Fielding, L., & Cassafer, G. (1991) *J. Biol. Chem. 266*, 12383–12394.

Clarke, D. M., Loo, T. W., Inesi, G., & MacLennan, D. H. (1989) *Nature 339*, 476–478.

Cleland, W. W. (1982) *Methods Enzymol. 87*, 159–179.

Coan, C. R., & Inesi, G. (1977) *J. Biol. Chem. 252*, 3044–3049.

Coan, C., & DiCarlo, R. (1990) *J. Biol. Chem. 265*, 5376–5384.

Coan, C., & Keating, S. (1982) *Biochemistry 21*, 3214–3220.

Coan, C., Verjovski-Almeida, S., & Inesi, G. (1979) *J. Biol. Chem. 254*, 2968–2974.

Coan, C., Amaral, J. A., & Verjovski-Almeida, S. (1993a) *J. Biol. Chem. 268*, 6917–6924.

Coan, C., Jakobs, P., Ji, J., & Murphy, A. J. (1993b) *FEBS Lett. 335*, 33–36.

de Meis, L., & Carvalho, M. C. G. (1974) *Biochemistry 13*, 5032–5037.

Dupont, Y. (1980) *Eur. J. Biochem. 109*, 231–238.

Dupont, Y. (1982) *Biochim. Biophys. Acta 688*, 75–87.

Eletr, S., & Inesi, G. (1972) *Biochim. Biophys. Acta 282*, 174–179.
Fernandez-Belda, F., Kurzmak, M., & Inesi, G. (1984) *J. Biol. Chem. 259*, 9687–9698.
Fujimori, T., & Jencks, W. P. (1992) *J. Biol. Chem. 267*, 18475–18487.
Highsmith, S., & Murphy, A. J. (1984) *J. Biol. Chem. 259*, 14651–14656.
Ikemoto, N., Garcia, A. M., Kurobe, Y., & Scott, T. L. (1981) *J. Biol. Chem. 256*, 8593–8601.
Inesi, G. (1987) *J. Biol. Chem. 262*, 16338–16342.
Inesi, G, & Landgraf, W. C. (1970) *Bioenergetics 1*, 355–365.
Inesi, G., Kurzmack, M., Coan, C., & Lewis, D. (1980) *J. Biol. Chem. 255*, 3025–3031.
Inesi, G., Lewis, D., Nikic, D., Hussain, A., & Kirtley, M. E. (1992) in *Advances in Enzymology and Related Areas of Molecular Biology* (Meister, A., Ed.) Vol. 65, pp 185–215, John Wiley and Sons, Inc., New York.
Jencks, W. P. (1992) *Ann. N.Y. Acad. Sci. 671*, 49–57.
Jencks, W. P., Yang,T., Peisach, D., & Myung, J. (1993) *Biochemistry 32*, 7030–7034.
Lewis, S. M., & Thomas, D. D. (1992) *Biochemistry 31*, 7381–7389.
Lowry, O. H., Rosenbrough, N. J., Farr, A. L., & Randall, R. J. (1951) *J. Biol. Chem. 193*, 265–275.
McIntosh, D. (1992) *J. Biol. Chem. 267*, 22328–22335.
McIntosh, D. B., Ross, D. C., Champeil, P., & Guillian, F. (1991) *Proc. Natl. Acad. Sci. U.S.A. 88*, 6437–6441.
Meszaros, L. G., & Bak, J. Z. (1993) *Biochemistry 32*, 10085–10088.
Nakamura, J. (1987) *J. Biol. Chem. 262*, 14492–14497.
Orlowski, S., & Champeil, P. (1991) *Biochemistry 30*, 11331–11342.
Penefsky, H. S. (1977) *J. Biol. Chem. 252*, 2891–2899.
Petithory, J. R., & Jencks, W. P. (1988a) *Biochemistry 27*, 5553–5564.
Petithory, J. R., & Jencks, W. P. (1988b) *Biochemistry 27*, 8626–8635.
Pickart, C. M., & Jencks, W. P. (1982) *J. Biol. Chem. 257*, 5319–5322.
Reinstein, J., & Jencks, W. P. (1993) *Biochemistry 32*, 6632–6642.
Ross, D. C., Davidson, G. A., & McIntosh, D. B. (1991) *J. Biol. Chem. 266*, 4613–4621.
Serpersu, E. H., Kirch, U., & Schoner, W. (1982) *Eur. J. Biochem. 122*, 347–354.
Scott, T. L. (1985) *J. Biol. Chem. 260*, 14421–14423.
Squire, T. C., Bigelow, D. J., de Ancos, J. G., & Inesi, G. (1987) *J. Biol. Chem. 262*, 4748–4754.
Squire, T. C., Bigelow, D. J., Franandez-Belda, F., de Meis, L., & Inesi, G. (1990) *J. Biol. Chem. 265*, 13713–13720.
Stahl, N., & Jencks, W. P. (1987) *Biochemistry 26*, 7654–7667.
Sumbilla, C., Cantilina, T., Collins, J. H., Malak, H., Lakowitz, J. R., & Inesi, G. (1991) *J. Biol. Chem. 266*, 12682–12689.
Tanford, C., Reynolds, J. A., & Johnson, E. A. (1987) *Proc. Natl. Acad. Sci. U.S.A. 84*, 7094–7098.
Thorley-Lawson, D. A., & Green, N. M. (1973) *Eur. J. Biochem. 40*, 403–413.
Vilsen, B., & Andersen, J. P. (1986) *Biochim. Biophys. Acta 898*, 313–322.
Vilsen, B., & Andersen, J. P. (1987) *Biochim. Biophys. Acta 898*, 313–322.
Vilsen, B., & Andersen, J. P. (1992a) *J. Biol. Chem. 267*, 3539–3550.
Vilsen, B., & Andersen, J. P. (1992b) *J. Biol. Chem. 267*, 6745–6751.
Wawrzynow, A., Collins, J. H., & Coan, C. (1993) *Biochemistry 32*, 10803–10811.